Final Report
Inelastic neutron scattering in valence fluctuation compounds
DE-FG02-03ER46036 for the period February 2006 through February 2011
PI: Jon Lawrence, Department of Physics and Astronomy, University of California, Irvine

Summary

The valence fluctuation compounds are rare earth intermetallics where hybridization of the nearly-localized 4*f* electrons with the conduction electrons leads to incorporation of the 4*f*'s into the itinerant states. This hybridization slows down the conduction electrons and hence gives them a heavy effective mass, justifying application of the term "heavy Fermion" (HF) to these materials. During the project period, we grew large single crystals of several such compounds and measured their properties using both standard thermodynamic probes and state-of-the-art inelastic neutron scattering. We obtained three main results. For the intermediate valence compounds $CePd_3$ and $YbAl_3$, we showed that the scattering of neutrons by the fluctuations of the 4*f* magnetic moment does not have the momentum dependence expected for the itinerant heavy mass state; rather, the scattering is more typical of a localized spin fluctuation. We believe that incoherent scattering localizes the excitation. For the heavy Fermion compound $Ce(Ni_{0.935}Pd_{0.065})_2Ge_2$, which sits at a $T = 0$ critical point for transformation into an antiferromagnetic (AF) phase, we showed that the scattering from the AF fluctuations does not exhibit any of the divergences that are expected at a phase transition. We speculate that alloy disorder profoundly suppresses the growth of the fluctuating AF regions, leading to short range clusters rather than regions of infinite size. Finally, we explored the applicability of key concepts used to describe the behavior of rare earth heavy Fermions to uranium based HF compounds where the 5*f* electrons are itinerant as opposed to localized. We found that scaling laws relating the spin fluctuation energy measured in neutron scattering to the low temperature specific heat and susceptibility are valid for the uranium compounds, once corrections are made for AF fluctuations; however, the degeneracy of the high temperature moment is smaller than expected for rare-earth-like Hund's rule behavior, essentially because the orbital moment is suppressed for itinerant 5*f* electrons. We also found that the standard local-moment-based theory of the temperature dependence of the specific heat, susceptibility and neutron scattering fails badly for URu_2Zn_{20} and UCo_2Zn_{20}, even though the theory is phenomenally successful for the closely related rare earth compound $YbFe_2Zn_{20}$. Both these results highlight the distinction between the itineracy of the 5*f*'s and the localization of the 4*f*'s. It is our hope that these results are sufficiently significant as to stimulate deeper investigation of these compounds.

Inelastic neutron scattering in valence fluctuation compounds
Jon Lawrence, University of California, Irvine

1 Introduction

In valence fluctuation (VF) rare earth compounds [1], nearly-localized rare earth 4f electrons hybridize with the conduction electrons. Because the 4f's have a small radial extent, the overlap with the conduction electrons is weak and the hybridization is small. In addition, there is a strong Coulomb repulsion when more than one electron attempts to occupy the site. This leads to a strongly correlated hopping in and out of the 4f orbitals, which hopping is sensitive to whether or not another electron is on the site. Under these circumstances, the high temperature state is that of a 4*f* local moment; at low temperatures, the band structure is renormalized to that of a hybridized, heavy mass Fermi liquid with the *f* electrons incorporated into the band. The characteristic temperature of the crossover between these two states is the Kondo temperature T_K. The occupancy of the 4*f* shell crosses over from an integral value at high *T* to a non-integral "intermediate" value at low *T*; the remainder is contributed to the valence band, which takes on an "intermediate" valence.

There are two important classes of VF materials: intermediate valence (IV) [2] and heavy Fermion (HF) compounds [3]. For IV compounds, the Kondo temperatures are large (T_K > 100 K), the valence is nonintegral (n_f < 0.9), and the masses are moderately enhanced (m^* ~ 10-50 m_e). The IV compounds exhibit a hybridization gap; they include Fermi liquids and the so-called Kondo insulators. For the HF compounds, the Kondo temperatures are small (T_K ~ 10 K), the *f*-occupancy n_f is close to unity (so that the *f*-electrons are nearly localized), and the masses are very large (m^* > 100 m_e). The HF compounds occur in the vicinity of a quantum critical point (QCP) for a $T = 0$ transition between a Fermi liquid (FL) ground state with large effective masses and a reduced moment (< 0.1 μ_B) magnetically ordered state; "marginal" Fermi liquids and non-*s*-wave superconductors are ubiquitous near the QCP.

The rich physics of the VF compounds presents a major unsolved correlated electron problem. Indeed, study of these compounds can contribute to the general understanding of strongly correlated electron systems, which category includes the high-T_c oxides and other modern materials of high current interest.

Because the *2J+1* magnetic degrees of freedom of the localized 4*f* electrons are absorbed into the itinerant electron states, resulting in highly renormalized, correlated electron states, the spin dynamics are crucial for our understanding of these materials. To this end, the appropriate tool is inelastic neutron scattering, which can resolve the dependence of the spin fluctuations on both the momentum (***Q***) and energy transfer (ΔE). The number of VF systems where experiments have been carried out on single crystals (required to establish the ***Q***-dependence) is, however, not very large. This is due both to the difficulty of growing the large crystals required for the inelastic measurement, and to the fact that several important examples contain strong neutron absorbers. The focus of our research has been to perform inelastic neutron scattering experiments on single crystals of IV and HF compounds that have not been studied previously in this manner.

2 Lack of *Q*-dependence in the Kondo scale scattering in the intermediate valence compounds $CePd_3$ and $YbAl_3$

A general belief is that the Anderson lattice (AL) model [4] should capture much of the essential physics of IV compounds. This model includes background conduction electrons with bandwidth *W*, a lattice of highly localized 4*f* electrons with an energy E_f required to excite the 4*f* into the conduction band, hybridization *V* between the 4*f* and the conduction electrons, and a Coulomb correlation energy *U* when more than one electron is on the site. Intermediate valence (IV) behavior occurs when the hybridization *V* is moderately large relative to E_f and *W*. In this case, a renormalized band structure with a small (~10-50 meV) hybridization gap occurs at low temperatures, similar to the band structure that occurs when a dispersionless level crosses a broad conduction band (Fig. 1a, inset) but with parameters that are strongly reduced (renormalized) due to the Coulomb correlations. When the Fermi level is in the gap, the compounds behave as small-gap semiconductors, i.e. as "Kondo insulators." When the Fermi level lies in the region of high density-of-states (DOS) near the zone boundary, the behavior is that of a moderately heavy mass Fermi liquid (i.e., metal).

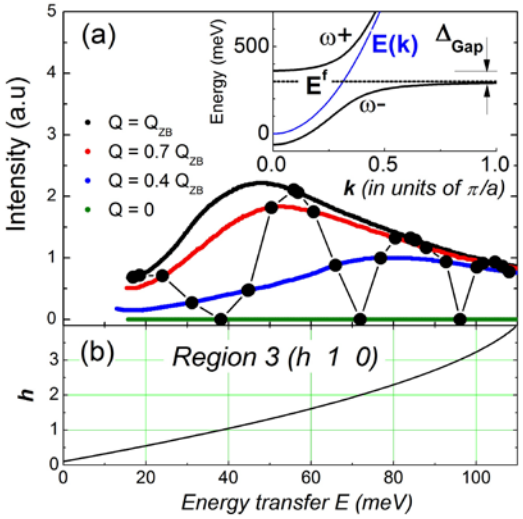

Fig.1: Inset: Showing the hybridized bands ω^+ and ω^- (solid lines) that arise when a dispersionless band (dashed line) crosses a parabolic conduction band (blue line). a) Spectra calculated [5] for the Anderson lattice for interband excitations for momentum transfer in the range between 0 and $Q = Q_{ZB}$. (b) The variation of the *H* component of reduced momentum transfer with energy transfer for the MAPS measurement for ($H(\Delta E)$, 1, 0), where *H* varies with energy transfer ΔE. Symbols are drawn on the spectra of (a) at the energies where *H(E)* takes on the (reduced) value of *Q* appropriate to each spectrum; the thin line is a smooth interpolation between these symbols.

In the renormalized band structure of Fig. 1, the neutron scattering intensity should be proportional to the "joint density of states"

$$\int N_i(\varepsilon_q)\, f(\varepsilon_q)\, N_f(\varepsilon_{q-Q})\, f(\varepsilon_{q-Q})\, d\varepsilon_q \qquad (1)$$

where $\varepsilon_{q-Q} - \varepsilon_q = \Delta E$ is the energy transfer, *Q* is the momentum transfer, *f* is the Fermi function and N_i and N_f are the initial and final densities of states. In calculations for the Anderson lattice (Fig. 1a), such scattering is highly *Q*-dependent. The most intense scattering occurs when the energy transfer ΔE equals the threshold for indirect transitions between the regions of large density of states at the zone center and zone boundary of the upper and lower bands respectively; this occurs for zone boundary momentum transfer $Q = q_{BZ}$ and for energy essentially equal to the Kondo energy $k_B T_K$. At smaller *Q*, the scattering should be weaker, with most of the spectral weight at much higher energies. (Fig. 1)

2a Experiments in $CePd_3$

The cubic ($AuCu_3$) intermetallic $CePd_3$ is a classic IV compound with a Kondo temperature of order 700 K, and strong mixed valence ($n_f \sim 0.8$) [6]. To explore the ***Q***-dependence of the spectra, we grew a large (20 gram) crystal via the Czochralski method and measured the spectra using the MAPS spectrometer at ISIS. We used the isostructural compound $LaPd_3$ to determine the nonmagnetic scattering. A low temperature spectrum is shown in Fig. 2. A broad peak of magnetic scattering is observed centered near E_{max} = 60 meV (the Kondo energy for this compound). Fig. 3 shows the ***Q***-dependence of the scattering for $\Delta E = E_{max}$ in the (K, L) plane. (These are Miller indices; i.e Q is expressed in reduced units $(a_0/2\pi)Q$.) It is clear that there is a maximum in intensity at the (K = 1/2, L = 0) zone boundary. In a time-of flight experiment performed on a chopper spectrometer such as MAPS at fixed angle between the sample and the beam, the Miller index H varies with energy transfer. For our spectra at (K = 1/2, L = 0), the value of H at ΔE = 60 meV is 1.5. Hence the bright spot in Figure 3 occurs at the (1/2, 1/2, 0) zone boundary point. This is initially encouraging, in that calculations for the Anderson lattice predict the strongest scattering should occur at the indirect threshold in energy (which should be the Kondo energy) and at the zone boundary.

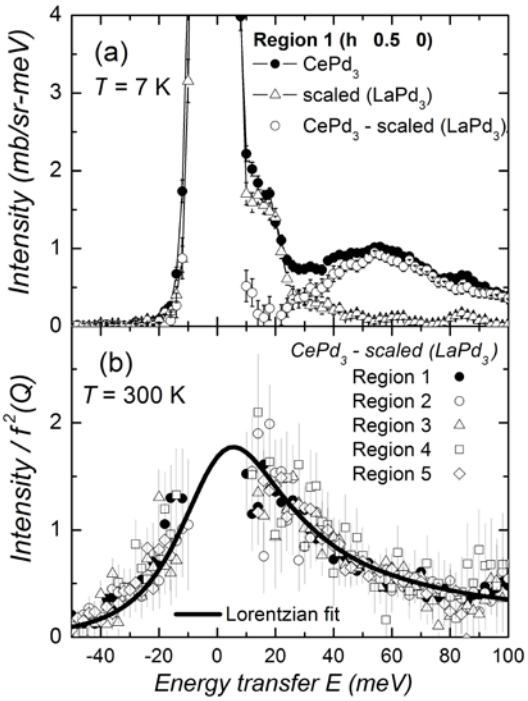

Fig. 2: Scattered intensity measured on the MAPS spectrometer with incident energy E_i = 120 meV. (a) Scattering at 7 K from the $CePd_3$ sample (black circles), scaled scattering from $LaPd_3$ (open triangles) and the difference (open circles), assumed to represent the magnetic scattering. The Q-values for these spectra are ($H(E)$, 0.5, 0). (b) Magnetic contribution to the scattering normalized by the magnetic form factor at five regions in Q-space at 300 K, and the corresponding quasielastic Lorentzian fit (black line).

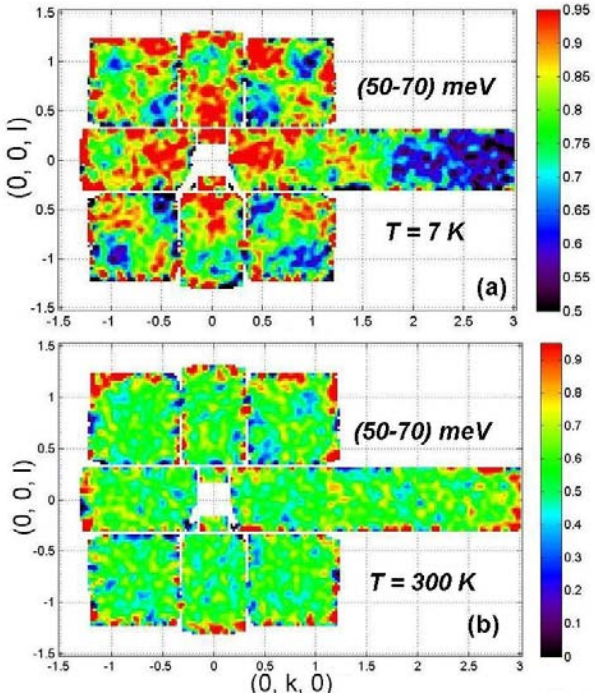

Fig. 3: Scattering intensity over the (K, L) plane integrated over an energy transfer range of 50 to 70 meV, for neutron scattering data taken on $CePd_3$ at 7 K (a), and at 300 K (b), using the MAPS spectrometer with incident neutron energy E_i = 120 meV. The color scale gives the intensity in mb/sr-meV units.

To proceed further, we divide the (*K*, *L*) scattering plane into regions, integrate over *K* and *L* around the centroid of each region, and take advantage of the four-fold cubic symmetry by adding equivalent regions to increase statistics. We divide out the 4*f* form factor so that all *Q*-dependence will represent differences within the Brillouin zone. As shown in Fig. 2b, the scattering at 300 K for five regions can be fit with a single quasielastic function, i.e., $\chi''(\Delta E) \sim \Delta E/(\Delta E^2 + \Gamma^2)$, with $\Gamma = 23.3$ meV. These room temperature spectra are clearly independent of *Q*, as can be seen as well for the scattering near $\Delta E = 60$ meV in Fig. 3b. While the existence of *Q*-independent quasielastic scattering in the high temperature state of an IV compound has been a general expectation for many years, this is the first time it has been directly established in a single crystal.

In Fig. 4, we exhibit the scattering for regions 1-3 centered at (*K*, *L*) = (1/2, 0), (1/2, 1/2) and (1, 0) respectively. The plot includes the dependence of the Miller index *H* on energy transfer for all three regions. The scattering in region 1 (*H*(*ΔE*), 1/2, 0) traverses the middle of the cubic zone face; the scattering in region 2 (*H*(*ΔE*), 1/2, 1/2) traverses an edge, and the scattering in region three (*H*(*ΔE*), 1, 0) runs from the center of the cube to the (1/2, 0, 0) zone boundary point. Consistent with Fig. 3a, the scattering at $\Delta E = 60$ meV is most intense in region 1. The scattering in region 2 shows oscillations in intensity along the zone edge, suggesting minima at the zone corner (1/2, 1/2, 1/2) and maxima at the middle of the edge (1/2, 1/2, 0). The scattering in region 3 is slightly less intense but is very similar in energy dependence to that of region 1.

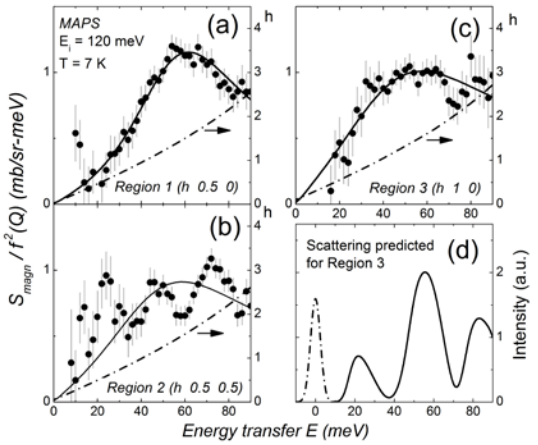

Fig. 4: (a,b,c) Magnetic contribution ($I(CePd_3)$ - 0.7 $I(LaPd_3)$) to the spectra normalized by the magnetic form factor (black circles) at three regions in the (*K*, *L*) plane, from measurements on MAPS. The black lines are fits to an inelastic Lorentzian power spectrum. The *H* component of *Q* is shown for each region as a dashed-dot line. (d) Magnetic contribution to the scattering (solid line) expected for region 3 based on the calculations shown in Fig. 1, after convolution with the instrumental resolution for the MAPS measurements.

This latter observation reveals an important difference with the predictions of the Anderson lattice, where the scattering on this energy scale should essentially vanish whenever $\boldsymbol{Q} =$ (*H*(*ΔE*), 1, 0) is in the middle of the zone (Fig. 1a), i.e. at those energy transfers where *H*(*ΔE*) is an integer. To make this more graphic, at each energy transfer *ΔE* we interpolate between the theoretical spectra of Fig. 1a to obtain the scattering intensity for the value of *H*(*ΔE*) for region 3 (thin line in Fig. 1a). We then convolve with the MAPS energy resolution to obtain the spectra of Fig. 4d. The theoretical expectation for region 3, which has zeros at zone center points, is very different from the data for this region.

Indeed, the scattering seen in Fig. 4 can be summarized [7] as follows: the spectral shape $I(\Delta E)$ is essentially similar for all $\boldsymbol{Q}$, but there are modest (~ 25%) variations in intensity, with maximal intensity at (1/2, 1/2, 0), and minimum intensity at (1/2, 1/2,1 /2). If we ignore the 25% variations in intensity, then it is apparent that the spectra are much closer to the Q-independent spectra expected for the Anderson *impurity* model (AIM) that for those expected for the Anderson lattice. To make this more graphic, we fit the Q-averaged spectra to a Lorentzian, and then compare to the predictions of the AIM in Fig. 5. The experimental and theoretical spectra are identical at room temperature, and very similar at low temperature.

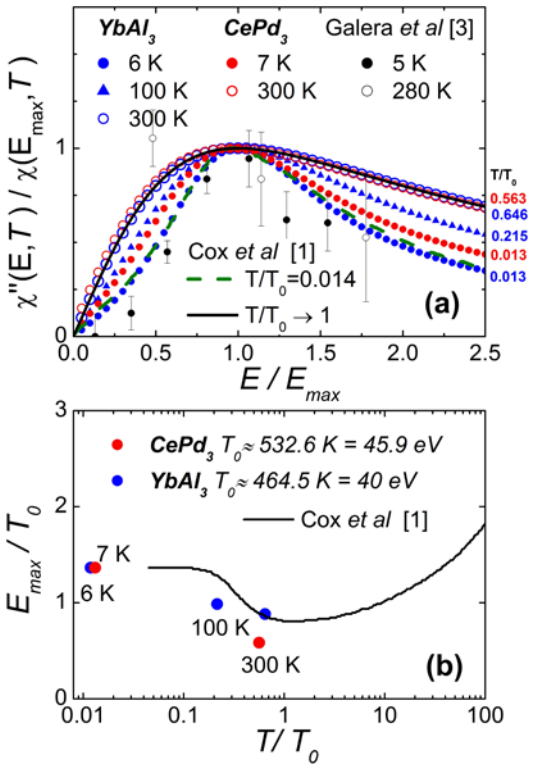

Fig. 5 Imaginary component of the dynamic susceptibility scaled by its peak value vs. energy scaled by the peak energy E_{max} for several temperatures. Fits from measurements on MAPS spectrometer for $YbAl_3$ (blue symbols) and $CePd_3$ (red symbols) are shown for comparison. AIM calculations [8] at low temperatures $T/T_0 = 0.014$ (dashed line) and the standard quasielastic behavior at $T=T_0$ (black line). (b) Temperature evolution of the energy of the peak of the dynamic susceptibility normalized by T_0. Calculation based on the AIM [8] (black line) and values obtained from INS on $CePd_3$ (red symbols) and $YbAl_3$ (blue symbols).

2b Experiments in $YbAl_3$

We grew large crystals of the IV compound $YbAl_3$ and, during the current project period performed high resolution inelastic scattering experiments on MAPS to complete the study of this compound begun earlier. There are two magnetic excitations observed in the range 10-100 meV. Kondo-scale scattering occurs as a broad Lorentzian peak centered near $\Delta E = E_{max} = 50$ meV. In addition, there is a narrow and highly Q-independent excitation at 30 meV, which we interpreted as a nearly-localized excitation at an energy lying within the hybridization gap. [9] Such an excitation has not been observed for other IV metals, and while the result is exciting, its origin is unclear. The Kondo-scale scattering exhibits a Q-dependence similar to that of $CePd_3$. In particular, as Q varies, the spectral shape does not change significantly but there are modest variations of intensity. [10] For this compound we found that the scattering was strongest near the (1/2, 1/2, 1/2) zone boundary point. As can be seen from Fig. 5, the averaged scattering (i.e. neglecting the modest intensity variations) exhibits both the spectral shape and temperature dependence expected for the Anderson impurity model.

2c Discussion of scattering in IV compounds

Our basic result for the Kondo-scale scattering in the IV compounds $CePd_3$ and $YbAl_3$ is that the *Q*-dependence is very different from that expected on the basis of the Anderson lattice, which is the "standard model" for IV compounds. While the scattering does show intensity maxima at certain zone boundary points, overall there is far less *Q*-dependence than expected on the basis of the model. In particular, the strong suppression of the Kondo scale scattering for $Q \rightarrow 0$ is not observed in the data. We note that similar results were observed in the 1990's for the intermediate valence compound $YbInCu_4$ [11]; and we have recently re-analyzed data from the literature for the actinide heavy Fermion compound UPt_3 to show that the *Q*-dependence is equally modest [12]. Hence, weak *Q*-dependence of the Kondo scale scattering may be a general feature of such materials.

We believe that the origin of this discrepancy between theory and experiment lies in incoherent scattering. If, when the neutron excites an electron across the hybridization gap from the lower to the upper renormalized band of Fig. 1 inset, the resulting electron quickly scatters incoherently, the *Q*-dependence will be lost. Riseborough has shown that this can happen in photoemission when higher order scattering is included. The effect is to turn the neutron excitation into a nearly-local spin fluctuation similar to that of the Anderson impurity model.

2d Ongoing experiments in IV compounds

The above mentioned problem with time-of-flight spectra in 3D crystals – that the Miller index H depends on energy transfer, so that the spectra are not obtained at constant $\boldsymbol{Q}$ – can be circumvented by rotating the sample, as in a triple axis spectrometer. With modern spectrometers at high intensity sources, a series of spectra at different sample/incident beam angles can be obtained in a reasonable period of time, and the results then interpolated in a manner that *Q* is controlled. We have recently obtained such spectra for $CePd_3$ using the MERLIN spectrometer at ISIS [Experiment RB 1010214]. Our preliminary analysis confirms what we observed on MAPS, but with controlled values of *Q*: namely that the Kondo scattering is strongest at (1/2,1/2, 0), intermediate at (1/2, 0, 0) and (0, 0, 0) and weakest at (1/2, 1/2, 1/2).

We also have obtained time on the ARCS spectrometer at SNS (Experiment IPTS-4041 ORNL) to repeat this experiment, but in a different manner. In particular, we are collaborating with Ray Osborn of Argonne National Laboratory to perform the experiment in the "asynchronous rotation mode." In this mode, the sample is rotated continuously during the experiment, and each neutron that is counted is tagged with the sample/incident beam angle, allowing determination of the momentum transfer for each scattering event. During the course of time, the complete 4-dimensional ($\mathbf{Q}$,ΔE) space is surveyed, allowing for slices at constant *Q*, constant *E*, etc.

In this manner, we hope to improve on our existing results, and should be able to display constant *Q* spectra for the Kondo-scale scattering.

3 Lack of divergences at the quantum critical point in the heavy Fermion compound $Ce(Ni_{0.935}Pd_{0.065})_2Ge_2$

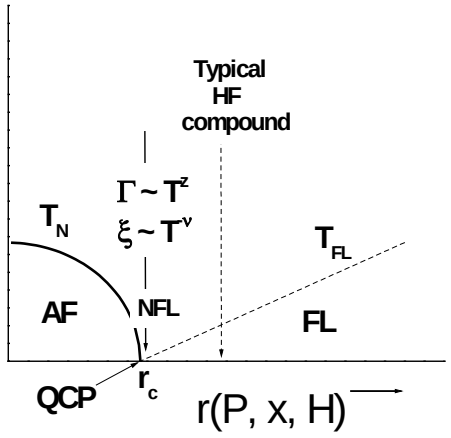

Fig. 6 Phase diagram with a quantum critical point

The low temperature physics of heavy Fermion compounds is dominated by proximity to a $T = 0$ quantum critical point (QCP) which separates a Fermi liquid (FL) from an antiferromagnetic (AF) ground state. [3] The antiferromagnetism is driven to a critical point at $T = 0$ by application of a control parameter r such as pressure P, alloy concentration x, or magnetic field H. Critical fluctuations of the AF order parameter give rise to a strong response in the neutron scattering near the Q vectors that correspond to the Bragg peaks $\boldsymbol{Q}_N$ of the nearby AF phase; this critical scattering is imposed on a background of Q-independent quasielastic scattering, which corresponds to the single site Kondo scattering. At the critical value of control parameter $r = r_c$, the correlation length, the lifetime τ of the critical fluctuations, and the staggered susceptibility are expected to diverge as $T \rightarrow 0$: $\xi \sim T^{-\nu}$, $\tau = h/\Gamma \sim \xi^z$, and $\chi(Q_N) \sim T^{-\gamma}$. For example, the SCR theory of Moriya and Takimoto [13], which is a weak coupling theory of an antiferromagnetic instability in a three dimensional Fermi liquid, gives the values $\gamma = 3/2$, $\nu = 3/4$, and $z = 2$.

A typical paramagnetic HF compound resides close to, but not quite at, the QCP and experiences critical AF fluctuations that grow increasingly strong as $T \rightarrow 0$. However, below the Fermi liquid temperature T_{FL} the staggered susceptibility, correlation length and the lifetime of the fluctuations saturate to finite values. The critical fluctuations contribute non-Fermi liquid (NFL) powerlaw behavior to the resistivity, specific heat and susceptibility in the paramagnetic state near the QCP.

The theory of the QCP was originally developed for the case of magnetic order in an itinerant electron system; i.e. for the case of a spin-density-wave instability at wavevector Q_N in a Fermi liquid (FL), such as the SCR theory. It has been argued [3] that the central issue for the QCP is whether it can be described by such a weak-coupling theory of a Fermi surface instability or whether there is a complete breakdown of Fermi liquid behavior associated with a crossover from localized to delocalized 4*f* electrons, and a concomitant new kind of critical behavior. The latter theories, with "local criticality," give E/T scaling for the spin fluctuations near the QCP.

3a Experiments in $Ce(Ni_{1-x}Pd_x)_2Ge_2$

A QCP exists in the alloy $Ce(Ni_{1-x}Pd_x)_2Ge_2$ at a critical concentration $x_c = 0.065$ [14]. We grew a 10 gram single crystal by the Czochralski method, using Ni-58 to decrease the incoherent scattering. The specific heat and resistivity of our crystal vary as $C/T = \gamma_0 - aT^{1/2}$ and the resistivity varies as $\rho = \rho_0 + bT^{3/2}$. We note that these are the predicted [13] powerlaws for SCR theory for a 3D antiferromagnetic QCP.

In order to explore the critical behavior, we measured the inelastic scattering on three spectrometers: SPINS and MACS at NIST and CNCS at SNS. The low energy ($0.3 < \Delta E < 2$ meV) spectra show two features (Fig. 7a): a broad, Q-independent peak centered near $\Delta E = 1.5$ meV and a lower energy feature that is highly Q-dependent, peaked near (H, K, L) = (1/2, 1/2, 0) (Fig. 8). The former represents the Kondo scattering ($T_K \sim 17$K) and the latter the critical fluctuations with $\boldsymbol{Q}_N$ = (1/2, 1/2, 0).

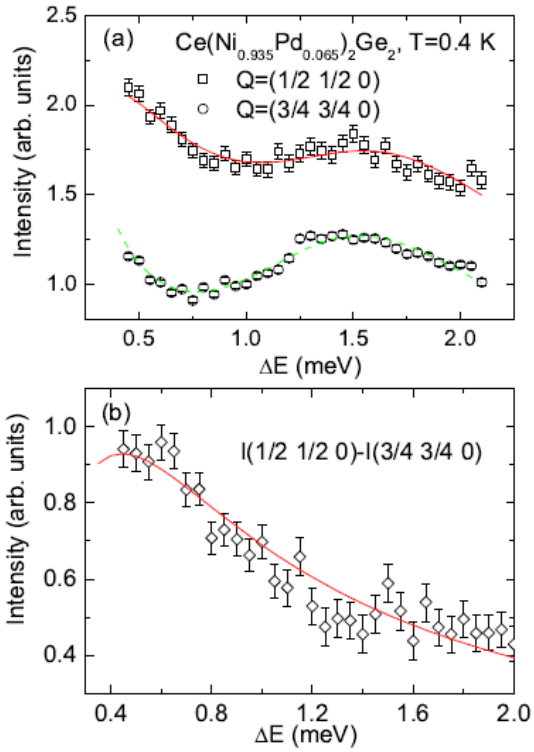

Fig. 7 a) Inelastic scattering of $Ce(Ni_{0.935}Pd_{0.065})_2Ge_2$ determined on SPINS at two Q. b) The difference between the two spectra.

To determine the spectra of the critical fluctuations, we subtract the Q-independent feature, as in Fig. 7b. For $Q = Q_N$, the spectra so obtained can then be fit with a quasielastic function

$$\chi''(\Delta E, Q_N) \sim \chi(Q_N) * \Delta E * \Gamma / (\Delta E^2 + \Gamma^2)$$

where $\chi(Q_N)$ is the staggered susceptibility and Γ is the inverse correlation lifetime. From fits to this formula (Fig. 9) we can extract the temperature dependence of the staggered susceptibility and the correlation time. The result is shown in Fig. 10, where it can be seen that

$$\Gamma \sim \Gamma_0 + \alpha\, T^{1.52}$$

and the staggered susceptibility varies as

$$\chi(Q_N)^{-1} \sim \chi(Q_N; T=0)^{-1} + \beta\, T^{1.43}.$$

These are to be compared to the predictions of the SCR theory:

$$\Gamma \sim \alpha\, T^{3/2} \text{ and } \chi(Q_N)^{-1} \sim \beta\, T^{3/2}$$

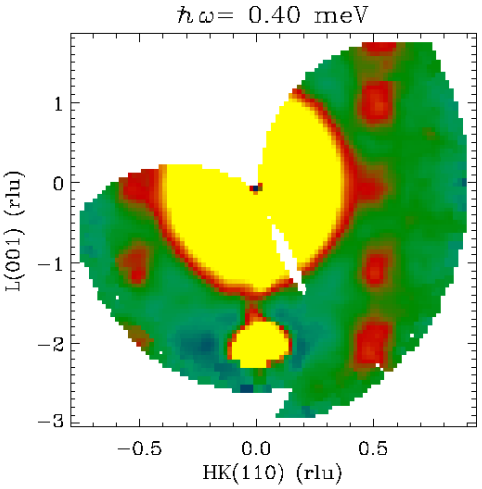

Fig.8 Inelastic scattering at an energy transfer 0.4 meV measured on MACS as a function of Q in the (H, H, L) plane. Bright red spots at (1/2, 1/2, L) arise from critical fluctuations.

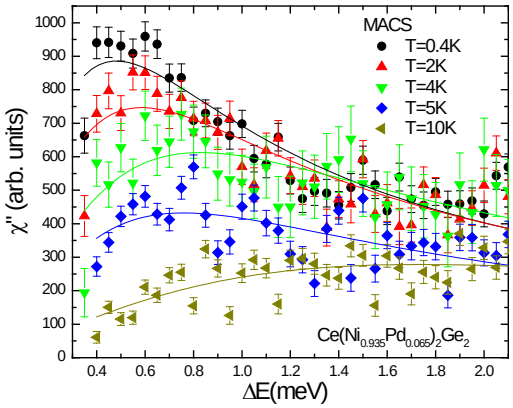

Fig.9 Fits of the critical scattering determined for $Ce(Ni_{0.935}Pd_{0.065})_2Ge_2$ using MACS to the quasielastic functional form at five temperatures.

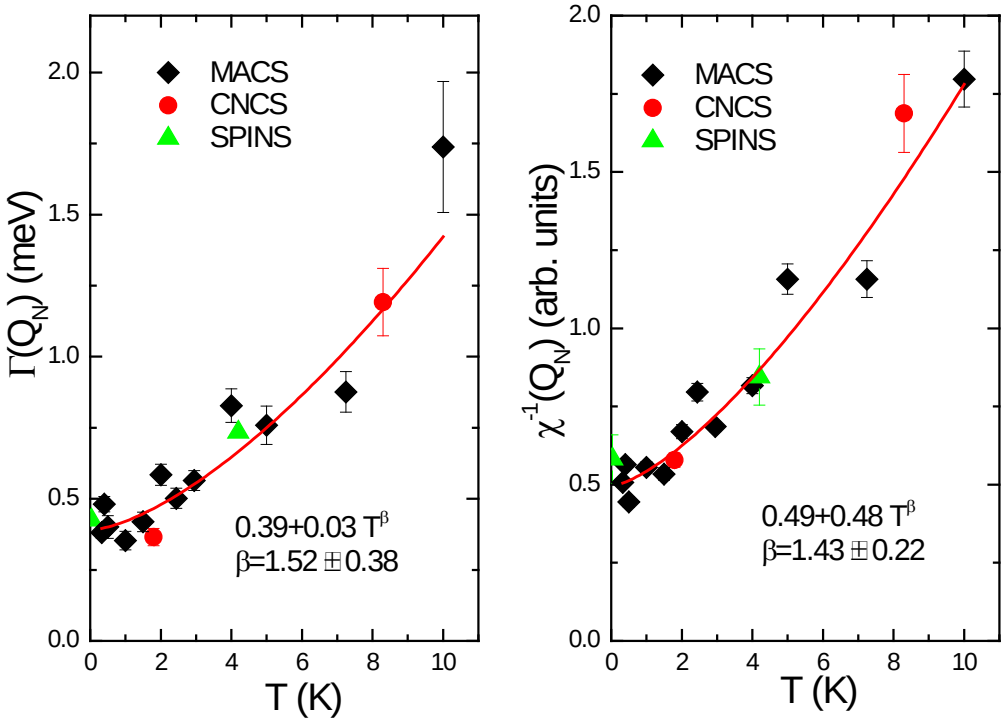

Fig. 10 a) The inverse correlation lifetime and b) the staggered susceptibility of $Ce(Ni_{0.935}Pd_{0.065})_2Ge_2$ as determined from measurements similar to those of Figs. 7 and 9 carried out on three spectrometers (SPINS, MACS, and CNCSMACS, and CNCS).

Hence the behavior of the specific heat, resistivity, correlation lifetime, and staggered susceptibility show a strong similarity to the predictions of the SCR theory. This suggests that the QCP is governed by an AF instability in a Fermi liquid and not by "local criticality." There is a very important caveat, however: neither the staggered susceptibility nor the correlation lifetime diverge. We have also measured the inverse coherence length $\kappa(T)$, by fitting the Q-dependence of the scattering at $\Delta E = \Gamma(T)$ to the Lorentzian formula

$$\chi''(\Delta E=\Gamma,Q)\sim \chi'(Q_N)^* [(\kappa/\pi)/((Q-Q_N)^2 + \kappa^2)].$$

We find that the coherence length does not diverge at low temperature, but also saturates to a finite value.

This lack of divergence at the critical point is contrary to all expectations about critical behaviour, but it is fairly ubiquitous in HF compounds alloyed to a QCP; for example, it is also observed in $Ce_{1-x}La_xRu_2Si_2$ [15] and $Ce(Ru_{1-x}Rh_x)_2Si_2$ [16] at the critical concentration x_c. Current speculation is that such behaviour is associated with a strong coupling between the quantum critical behaviour and alloy disorder. The alloy parameter drives the system into the AF phase by reducing the Kondo temperature, but at $x = x_c$, alloy disorder gives rise to a distribution of Kondo temperatures, and hence to finite size clusters, some nonmagnetic and some antiferromagnetic. Only those clusters that are truly critical and that percolate to infinite length will contribute to the expected divergences [17], and these have a small spectral weight compared to the regions which are not critical.

4 "Kondo-esque" behaviour of the spin fluctuations in uranium-based heavy Fermion intermetallic compounds

Our results for $CePd_3$ and $YbAl_3$ exhibited in section 2 are consistent with a larger body [18, 19] of results which suggest that the Kondo/Anderson *impurity* model (K/AIM) gives a good description of the behavior of the specific heat C_p, 4f occupation number n_f, susceptibility χ, and neutron scattering spectra $\chi''(\Delta E)$ of rare earth intermediate valence compounds. For some compounds, such as $YbAgCu_4$ [18] and $YbFe_2Zn_{20}$ [20], the fits of the K/AIM to the data are very precise; for others, the impurity theory gives good but semi-quantitative agreement with experiment. This can be viewed as a surprising result, since the appropriate theory for these compounds where the 4*f* electrons sit on a periodic array should be the Anderson lattice model (ALM). The two models are particularly different in the low temperature state where the K/AIM exhibits a localized Kondo resonance, while the ALM exhibits coherent renormalized hybridized bands. The basic condition for this agreement of the data with an impurity model is that the experimental properties (C_p, n_f, χ, and $\chi''(E)$) are dominated by spin fluctuations which are essentially local. As we argued above, the weak Q-dependence of the neutron spectra indicates that this is indeed the case.

We have begun a series of experiments to see how this scenario plays out for uranium-based heavy Fermion compounds. The Kondo/Anderson model, whether for an impurity or for a lattice, assumes localized (dispersionless) electrons. The 4*f* electrons are indeed highly localized, but the 5*f* electrons in the actinides show all the signs expected for itinerant behavior. The question then arises: how appropriate is the K/AIM for describing heavy Fermion behavior in actinide compounds? More generally, what differences are there in the heavy Fermion behavior of the actinides and the rare earths due to the itineraacy of the 5*f*'s in the former and the localization of the 4*f*'s in the latter?

4a Kondo-esque scaling in heavy Fermion uranium-based paramagnets

In the rare earth (RE) IV compounds, the primary spin fluctuation (whose spectrum is typically a broadened Lorentzian) gives rise, when excited, to the high temperature moment. Such an excitation is seen not only in IV compounds but in RE heavy Fermion compounds – e.g. the 1.5 meV excitation observed in $Ce(Ni_{0.935}Pd_{0.065})_2Ge_2$ in Fig. 7a is such a fluctuation – and a similar primary fluctuation is seen in all HF uranium intermetallics. Because the K/AIM theory works so well to describe the relationship of this fluctuation to the thermodynamics in the RE IV compounds, we will refer to this primary spin fluctuation as "Kondo-esque."

One of the oldest-known properties of HF and IV materials, whether in uranium or in rare earth (RE) compounds, is the existence of a scaling law whereby the low temperature susceptibility $\chi(0)$ and specific heat coefficient $\gamma = C/T$ vary with the inverse $1/T_{sf}$ of the characteristic energy $k_B T_{sf}$ of the primary spin fluctuation [1]. The latter quantity can be equated to the maximum E_{max} in the dynamic susceptibility $\chi''(E)$ measured through inelastic neutron scattering. In Fig. 11, we compare the susceptibility, specific heat, and neutron spectra of two related compounds, URu_2Zn_{20} and UCo_2Zn_{20} [21]. The zero temperature susceptibility and specific heat coefficient of the latter compound are approximately three times larger, and the energy E_{max} of the maximum in the neutron spectra is three times smaller than in the former compound.

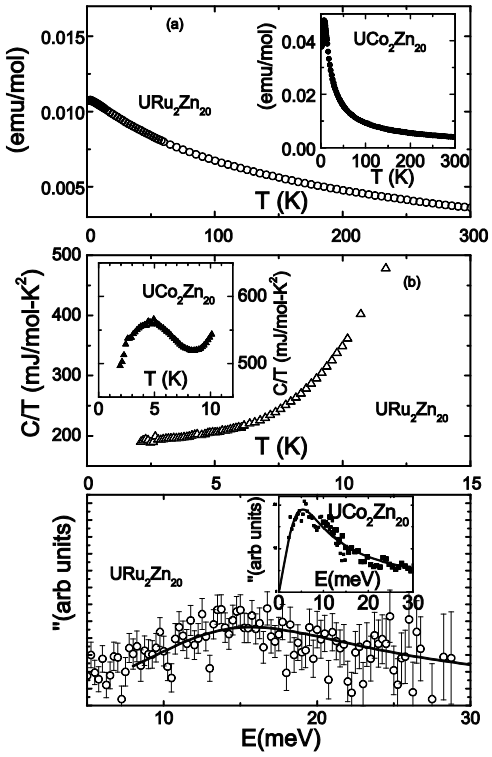

Fig. 11 (a) Susceptibility, (b) specific heat coefficient and (c) inelastic magnetic neutron scattering spectrum of URu_2Zn_{20}The insets show the same quantities for UCo_2Zn_{20} (Data from Ref. 21.)

The scaling laws arising from the primary spin fluctuation receive theoretical justification from the Kondo/Anderson impurity model where the spin fluctuation temperature T_{sf} is identified with the Kondo temperature T_K. While the K/AIM results in very precise scaling laws it assumes, as mentioned above, localized electrons. Since we are concerned with the applicability of scaling to itinerant 5*f* electrons, we first show that the low temperature scaling laws follow from very general considerations. The spin fluctuation peak at $E_{max} = k_B T_{sf}$ in the dynamic susceptibility represents an excitation of the 4*f* or 5*f* moment out of a singlet (non-magnetic) ground state. The excited level has the degeneracy of the local 4*f* (or itinerant 5*f*) moment, which for rare earths is $N_J = 2J+1$. At high temperatures, the moment is excited; at low temperatures, the moment "freezes out" and the system is nonmagnetic.

A phenomenology of the scaling can be obtained [12] by making several simplifying approximations. The spin excitation at E_{max} will give rise to a peak in the specific heat at a temperature $T(C_{max})$ that is similar to a Schottky peak, with the exception that $C(T)$ is linear at low temperature for heavy Fermion compounds. (This linearity is related to the substantial breadth of the excitation.) If we assume that C is linear for $T < T(C_{max})$, that half the $R\ln(2J+1)$ entropy is generated between $T = 0$ and $T(C_{max})$, and that $T(C_{max})$ is approximately equal to $T_{sf}/3$ (a similar statement is true for both Schottky anomalies and for the Kondo specific heat), we then obtain $E_{max}\gamma = 3/2\ R\ln(2J+1)$ for the scaling constant. If we further assume that the susceptibility has a van Vleck-like form $\chi(0) \sim C_J / T_{sf}$ (where C_J is the free ion Curie constant for total angular momentum J) then we obtain the value $2\pi^2/(9\ln(2J+1))$ for the Wilson ratio $W = (\pi^2 R/(3\ C_J))*\chi(0)/\gamma$.

Clearly the scaling constants derived from this phenomenology can only be viewed as roughly approximate. The point of the exercise is that scaling laws with values similar to those of the K/AIM (Table 1) are expected on very general grounds, even when the spin fluctuations arise in an itinerant system where the K/AIM is not applicable. In particular, the phenomenology exhibits the strong dependence of $E_{max}\gamma$ on the degeneracy. As we will see, this will allow us to distinguish the cases of itinerant and local *f* electrons.

Table 1. Comparison of scaling constants deduced from Kondo theory and the rough phenomenology of the text.

J	$E_{max}\gamma$(Kondo)	$E_{max}\gamma$(Rough)	W(Kondo)	W(Rough)
	$(\pi/3)RJ$	$(3/2)\ Rln(2J+1)$	$(1+(1/2J))$	$(2\pi^2/9)/ln(2J+1)$
3/2	13.0	17.3	1.33	1.58
5/2	21.8	22.3	1.20	1.22
7/2	30.4	25.9	1.14	1.05
9/2	39.1	28.7	1.11	0.95

In Table 2, we exhibit the experimental values of W and $E_{max}\gamma$ deduced from values of $\chi(0)$, γ. and E_{max} obtained from the literature. In this table, we compare the uranium HF compounds to the rare earth IV compounds, for the reason that the characteristic temperatures of the spin fluctuations are similar: they are typically 100 K or more, rather than ~ 10K as seen in the RE HF compounds. We include all paramagnetic compounds in these two categories for which all three of the quantities $\chi(0)$, γ. and E_{max} have been reported. It can be seen that the low temperature scaling works well for J = 5/2 cerium and J = 7/2 ytterbium IV compounds. Low temperature scaling also works well for URu_2Zn_{20} and UCo_2Zn_{20} under the assumption that the high temperature moment is that of a Hund's Rule $5f^2$ or $5f^3$ electron. For other classic uranium heavy Fermion compounds such as UAl_2, USn_3, UPt_3, and UBe_{13} one or the other of the two scaling constants is unacceptably different (a factor of two or more) from the value expected for the Hund's rule moment.

Table 2 Low temperature scaling constants for Ce (J = 5/2), Yb (J = 7/2), and U (J = 4, 9/2 or undetermined) compounds. Rows marked "Corrected" use the technique described in the text to correct for the AF fluctuation contribution to the specific heat. From Ref. 12.

Compound	γ(J/mol-K^2)	$\chi(0)$ (emu/mol)	E_{max}(K)	γE_{max}(J/mol-K)	Wilson ratio
$CePd_3$	0.035	0.0018	638	22.3	1.74
$CeSn_3$	0.042	0.0018	464	19.5	1.49
$YbAl_3$	0.04	0.005	634	25.4	1.32
$YbInCu_4$	0.041	0.006	466	19.1	1.54
$YbAgCu_4$	0.199	0.017	133	26.5	0.9
$YbFe_2Zn_{20}$	0.52	0.05	70	36.4	1.02
UAl_2	0.14	0.004	243	34.0	0.48
(Corrected)	0.07			17.0	1.30
USn_3	0.17	0.01	60	10.2	0.99
URu_2Zn_{20}	0.188	0.012	191	35.9	1.08
UPt_3	0.45	0.009	58	26.1	0.34
(Corrected)	0.225			13.0	1.10
UCo_2Zn_{20}	0.558	0.047	70	39.1	1.42
UBe_{13}	1.1	0.015	150	165	0.23
(Corrected)	0.183			27.4	1.38

The latter compounds typically reside close to a quantum critical point (QCP) for a $T = 0$ transition to a magnetic state, where antiferromagnetic (AF) fluctuations representing critical scattering close to the phase transition also occur. Both the primary fluctuation and these AF fluctuations contribute to the specific heat. In particular, the AF fluctuations cause an upturn at low temperature in the specific heat coefficient, C/T. One way to subtract this contribution is to extrapolate from higher temperature. This is shown for UBe_{13} in Fig. 12. If we use the extrapolated value for the specific heat coefficient, $\gamma_{ext} = 0.183$ J/mol-K^2 instead of the low temperature value $\gamma_{LowT} = 1.1$ J/mol-K^2 then the scaling constants become $E_{max}\gamma = 27$ and $W = 1.4$, which values are much more consistent with expectations for Kondo-esque scaling than the uncorrected values $E_{max}\gamma = 165$ and $W = 0.23$.

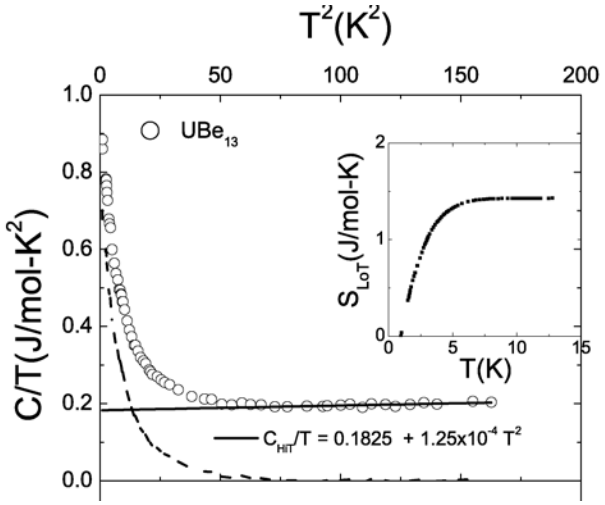

Fig. 12 The specific heat coefficient of UBe_{13} plotted versus the square of the temperature. The solid line extrapolates from higher temperature; the dashed line is the excess over the extrapolation. The entropy of the excess is shown in the inset; note that the entropy generated is a small fraction of the expected total R ln 10. Analysis from Ref. 12.

If we attempt a similar correction for UAl_2 or UPt_3, we find that the scaling constant $E_{max}\gamma$ is then too small. This is connected to the fact that the high temperature Curie constants in these compounds are closer to the value 1 emu-K/mol than to the value 1.6 emu-K/mol expected for a $5f^2$ or $5f^3$ Hund's rule multiplet. The point is that the angular momentum is typically quenched for itinerant electrons. This leads to a smaller degeneracy and Curie constant than expected for the Hund's rule configuration. The expected $E_{max}\gamma$ scaling constant, which depends strongly on the degeneracy, is also reduced. This is the main way in which the itineracy of the 5*f* electrons shows up in the scaling analysis [12].

The results allow us to formulate a line for future research: First, the quantities C_p, $\chi(T)$, and $\chi''(Q,E)$ should be measured in a single crystal of a given compound. As we showed above for $Ce(Ni_{0.935}Pd_{0.065})_2Ge_2$, the Kondo-esque and AF fluctuation contributions to $\chi''(Q,E)$ can then be separated. The spectral weight of these two contributions to the magnetic neutron scattering should then be correlated with the fractional entropy of each contribution to the specific heat. Second, the absolute cross section of the primary spin fluctuation should be measured and the appropriate sum rule used to see whether the integrated scattering corresponds to the high temperature moment seen in the susceptibility. Third, the primary spin fluctuation needs to be measured on single crystals of uranium compounds in an effort to clarify whether the *Q*-dependence of this excitation is localized or delocalized in the low temperature state.

4b Comparison of the behavior of URu_2Zn_{20}, UCo_2Zn_{20}, and $YbFe_2Zn_{20}$ to the K/AIM

From the preceding we see that the unranium intermetallic HF paramagnets obey Kondo-esque scaling laws with the key difference to the scaling behavior of the rare earth IV compounds being the reduced degeneracy of the high temperature moment due to the itineracy. Exploration of the "1-2-20" system AB_2Zn_{20} (A = Yb, U; B = Ru, Co, Fe) [20,21,22], however, allows for a more direct examination of the degree to which the actinides and rare earth HF compounds follow Kondo/Anderson behavior.

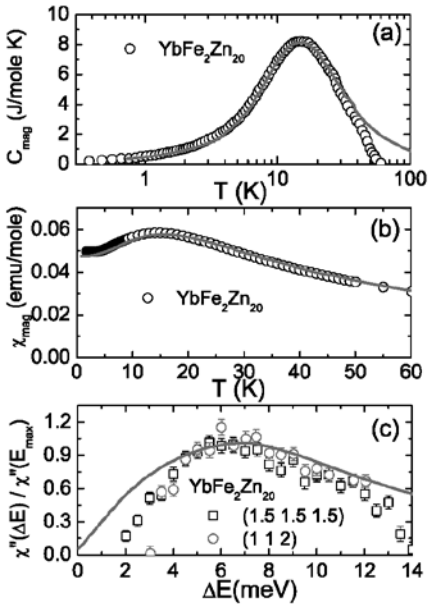

Fig. 13 The magnetic contribution to the specific heat, the susceptibility, and the inelastic neutron spectrum of $YbFe_2Zn_{20}$ compared to the predictions of the K/AIM.

both URu_2Zn_{20} and UCo_2Zn_{20} to the predictions of the K/AIM. While the Kondo scaling laws for a $J = 4$ or J = 9/2 moment are obeyed at low temperature (Tables 1 and 2), the fits deviate strongly as the temperature is raised, especially in comparison to the quality of the fits in $YbFe_2Zn_{20}$. In particular, the actual materials do not continue to develop entropy as rapidly as the model. While we do not understand this latter feature, we believe that the inability of the K/AIM to fit the data of these actinide compounds, even when the Kondo-esque scaling is obeyed at low temperature, is a consequence of the itineracy of the uranium 5*f* electrons.

As shown in Fig. 13, the compound $YbFe_2Zn_{20}$ is an example of a rare earth HF compound for which the K/AIM provides excellent fits to the susceptibility, specific heat, and inelastic neutron spectrum [21]. Comparison to Fig. 11 shows that the low temperature susceptibility is comparable in magnitude to that of UCo_2Zn_{20} (~ 0.05 emu-/mol) and a similar statement holds for the magnitude of the low temperature specific heat coefficient (which is ~ 0.5 J/mol-K^2 for both compounds) and for the position E_{max} ~ 6 meV of the peak in the inelastic neutron scattering. This raises the question: since the data for the rare earth HF compound $YbFe_2Zn_{20}$ is so well-represented by the K/AIM, is the same true for the actinide HF compound UCo_2Zn_{20}? The answer is shown in Fig. 14, where we compare the behavior of

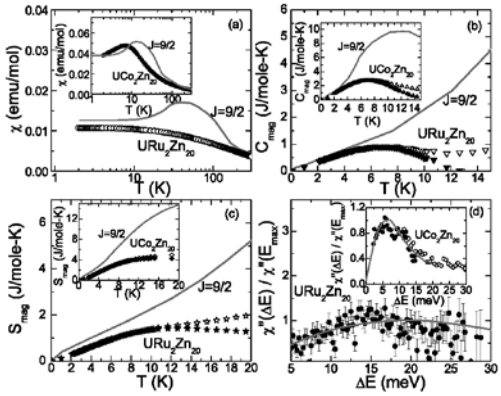

Fig. 14 Susceptibility, specific heat, entropy, and neutron scattering spectrum of URu_2Zn_{20} and UCo_2Zn_{20} (insets) compared to the predictions of the K/AIM.

5 Other experiments

5a Ce_3In/Ce_3Sn: These are heavy Fermion compounds with specific heat coefficients so large (0.7 and 0.3 J/mol-K^2 respectively) as to suggest proximity to a QCP. The magnetic fluctuations in this compound are known to be ferromagnetic (FM). We measured [23] the neutron spectra, the susceptibility $\chi(T)$ and the field dependence of the magnetization $M(H)$ and specific heat $C(H;T)$ on polycrystalline samples. We determined the crystal field ground state (and hence the low temperature g-factor) and the Kondo energy using neutron scattering. We then used this information to separate the measured behavior of $\chi(T)$, $M(H)$ and $C(H;T)$ into contributions from the Kondo effect, the crystal fields, and the FM correlations. We found that the FM correlations constituted a 10% contribution to the magnetization and entropy. If large single crystals became available, it would be possible to compare this to the fractional spectral weight of the FM correlations and the Kondo-esque scattering, as proposed above for uranium compounds at the end of section 4a. We point out here that such a separation requires both knowledge of the low-temperature g-factor and knowledge that the K/AIM is applicable -- which knowledge is not generally available for most uranium compounds.

5b The heavy Fermion compound $Ce_3Co_4Sn_{13}$: The compound $Ce_3Co_4Sn_{13}$ has an extremely large value of specific heat coefficient (4J/mol-K^2), indicating that it resides very close to a QCP. We grew large crystals and measured [24] the inelastic scattering on the SPINS spectrometer. We found that the Kondo scale was so small (of order 0.1 meV or less) that a higher-resolution spectrometer would be needed to characterize the scattering. We also measured [25] the diffraction in a magnetic field. We found that the magnetic field builds intensity in the (0, 0, 1) peak, which is not allowed in the crystal structure and thus represents antiferromagnetic fluctuations. The intensity tracks the magnetization, as though the strength of the AF fluctuations track the polarization of the 4f electrons – a rather strange result.

5c Itinerant magnetism in UMn_2Al_{20}: We grew crystals of several UT_2Al_{20} compounds in Al flux. For T = V, Mo, temperature independent Pauli paramagnetism is observed. For UMn_2Al_{20}, a ferromagnetic transition at T_c = 20K is observed. We measured $\chi(T)$, $M(H)$, $C(T)$, resistivity and the neutron scattering spectrum of this compound [26]. The specific heat peak at T_c is extremely small, and no anomaly is observed at T_c in the resistivity. We attribute the weakness of these anomalies to the onset of small moment ferromagnetism in an itinerant system.

5d Induced moment antiferromagnetism in Pr_3In: The compound Pr_3In, is an induced-moment incommensurate antiferromagnet below T_N = 12K. We measured the inelastic scattering of this compound on HRMECS and LRMECS at IPNS [27]. Above 100K, the data can be fit with the expected crystal field scheme, which shows a singlet-triplet excitation at 6 meV, but dispersion of the crystal field levels is strong below 100K. This is as expected based on the theory of induced magnetic order in a singlet-triplet system. We also measured [28] the magnetocaloric effect, and found that a phase transition occurs at B = 2T. We performed diffraction in a magnetic field on BT1 at NIST and found that the incommensurate AF structure is replaced by a $\boldsymbol{Q}$ = 0 structure above B = 2T. This either reflects ferromagnetic polarization of the Pr moments – which would be surprising given the small transition field relative the transition temperature – or a $\boldsymbol{Q}$ = 0 AF structure. The results undoubtedly reflect the presence of magnetic frustration on the fcc lattice.

References

1 J M Lawrence, P S Riseborough and R D Parks, Rep Prog Phys **44** (1981) 1.
2 J M Lawrence, Modern Physics Letters **22** (2008) 1273.
3 H. von Löhneysen *et al*, Rev Mod Phys **79** (2007) 1015.
4 A C Hewson. *The Kondo problem to heavy Fermions*. Cambridge University Press, 1993.
5 A A Aligia and B Alascio, J Mag Mag Mat **46** (1985) 321.
6 A P Murani *et al*, Phys Rev B 53 (1996) 2641.
7 V.R. Fanelli *et al*, arXiv: 0908.4378.
8 D L Cox *et al*, J Mag Mag Mat **54-57** (1985) 1.
9 A. D. Christianson *et al*, Physical Review Letters **96**, 117206 (2006).
10 Victor Fanelli, Ph D thesis, University of California, Irvine, 2009.
11 J M Lawrence *et al*, Phys Rev B **55** (1997) 14467.
12 J M Lawrence *et al*, Journal of Physics: Condensed Matter **23** (2011), to be published. arXiv: 1101.3992.
13 T Moriya and T Takimoto, Journ Phys Soc Japan **64** (1995) 960.
14 C H wang *et al*, Journal of Physics: Conference Series, to be published.
15 W Knafo *et al*, Phys Rev B **70** (2004) 174401.
16 H Kadowaki *et al*, Phys Rev B **96** (2006) 016401.
17 W Montfrooij *et al*, Phys Rev B 7**6** (2007) 052404.
18 J M Lawrence *et al* Phys Rev B **63** (2001) 054427.
19 A L Cornelius *et al*, Phys Rev B **88** (2002) 117201.
20 M S Torikachvili *et al*, Proc Natl Acad Sci USA **104** (2007) 9960.
21 C H Wang *et al*, Physical Review B **82**, (2010) 184407.
22 E D Bauer *et al*, Phys Rev B **78** (2008) 115120.
23 C H Wang *et al*, Physical Review B **81** (2010) 235132.
24 A D Christianson *et al*, Journal of Magnetism and Magnetic Materials, **310** (2007) 266.
25 A D Christianson *et al*, Physica B **403** (2008) 909.
26 C H Wang *et al*, Physical Review B **82** (2010) 094406.
27 A D Christianson et al, Journal of Applied Physics **101** (2007) 09D505.
28 V R Fanelli et al, Physica B **403** (2008) 1368.

Publications resulting from DOE Grant DE-FG02-03ER46036

1. Localized excitation in the hybridization gap in $YbAl_3$, A. D. Christianson, V.R. Fanelli, J.M. Lawrence, E. A. Goremychkin, R. Osborn, E. D. Bauer, J. L. Sarrao, J. D. Thompson, C. D. Frost and J.L. Zarestky, Physical Review Letters **96**, 117206 (2006).
2. Anisotropic intermediate valence in $Yb_2Rh_3Ga_9$, A. D. Christianson, J. M. Lawrence, A. M. Lobos, A. A. Aligia, E. D. Bauer, N. O. Moreno, E. A. Goremychkin, K.C. Littrell, J. L. Sarrao, J. D. Thompson, and C. D. Batista, Physica B, **378-80**, 752 (2006).
3. Observation of field induced single impurity behavior in the heavy Fermion compound $Ce_3Co_4Sn_{13}$, A.L. Cornelius, A.D. Christianson, J.M. Lawrence, V. Fritsch, E.D. Bauer, J.L. Sarrao, J.D. Thompson and P.G. Pagliuso, Physica B, **378-80**, 113 (2006).
4. Ytterbium divalency and lattice disorder in near-zero thermal expansion YbGaGe, C.H. Booth, A.D. Christianson, J.M. Lawrence, L.D. Pham, J.C. Lashley and F.R. Drymiotis, Physical Review B **75**, 012301 (2007).
5. Low temperature behavior of the heavy Fermion $Ce_3Co_4Sn_{13}$, A.D. Christianson, J.S. Gardner, H.J. Kang, J.-H. Chung, S. Bobev, J.L. Sarrao and J.M. Lawrence, Journal of Magnetism and Magnetic Materials, **310**, 266 (2007).
6. Crystal field excitations in the singlet ground state compound Pr_3In, A.D. Christianson, J.M. Lawrence, K.C. Littrell, E.A. Goremychkin, A.I. Kolesnikov, J.D. Thompson and J.L. Sarrao, Journal of Applied Physics **101**, 09D505 (2007).
7. Inelastic magnetic neutron scattering in $CePd_3$, J.M. Lawrence, V.R. Fanelli, E.A. Goremychkin, R. Osborn, E.D. Bauer, K.J. McClellan and A.D. Christianson, Physica B **403**, 783 (2008).
8. Neutron diffraction study of magnetic field induced behavior in the heavy Fermion $Ce_3Co_4Sn_{13}$, A.D. Christianson, E.A. Goremychkin, J.S. Gardner, H.J. Kang, J.-H. Chung, P. Manuel, J.D. Thompson, J.L. Sarrao,and J..M. Lawrence, Physica B **403**, 909 (2008).
9. Magnetic order in the induced magnetic moment system Pr_3In, V.R. Fanelli, A.D. Christianson, M. Jaime, J.D. Thompson, H.S. Suzuki and J.M. Lawrence, Physica B **403**, 1368 (2008).
10. Simplifying strong electronic correlations in uranium: Localized uranium heavy Fermion UM_2Zn_{20} (M = Co, Rh) compounds, E.D. Bauer, C. Wang, V.R. Fanelli, J.M. Lawrence, E.A. Goremychkin, N.R. de Souza, F. Ronning, J.D. Thompson, A. Silhanek, V. Vildosola, A.M. Lobos, A.A. Aligia, S. Bobev, and J.L. Sarrao, Physical Review B **101**, 115120 (2008).
11. Intermediate valence metals, J. M. Lawrence, Modern Physics Letters **22**, 1273 (2008).
12. Transition from heavy Fermion to mixed valence behavior in $Ce_{1-x}Y_xAl_3$: A quantitative comparison with the Anderson impurity model, E.A. Goremychkin, R. Osborn, I.L. Sashin, P. Riseborough, B.D. Rainford, D.T. Adroja, and J.M. Lawrence, Physical Review Letters **104**, 176402 (2010).
13. Kondo behavior, ferromagnetic correlations, and crystal fields in the heavy Fermion compounds Ce_3X (X = In, Sn), C.H. Wang, J.M. Lawrence, A.D. Christianson, E.A. Goremychkin, V.R. Fanelli, K. Gofryk, E.D. Bauer, F. Ronning, J.D. Thompson, N.R. DeSouza, A.I. Kolesnikov, and K.C. Littrell, Physical Review B **81**, 235132 (2010).
14. UMn_2Al_{20}: Small itinerant moment or induced local moment ferromagnetism, C.H. Wang, J.M. Lawrence, E.D. Bauer, K. Kothapalli, J.S. Gardner, F. Ronnong, K. Gofryk, J.D. Thompson, H. Nakotte, F. Trouw, Physical Review B **82**, 094406 (2010).

15. Neutron scattering and scaling behavior in URu_2Zn_{20} and $YbFe_2Zn_{20}$, C.H. Wang, A.D. Christianson, J.M. Lawrence, E.D. Bauer, E.A. Goremychkin, A. I. Kolesnikov, F. Trouw, F. Ronning, J.D. Thompson, M.D. Lumsden, N. Ni, E.D. Mun, S. Jia, P.C. Canfield, Y. Qiu, and J.R.D. Copley, Physical Review B **82**, 184407 (2010).
16. Crystal growth of CsCl-type $Yb_{0.24}Sn_{0.76}Ru$, T. Klimczuk, C. H. Wang, Q. Xu, J. Lawrence, T. Durakiewicz, F. Ronning, A. Lobet, E.D. Bauer, J-C. Griveau, W. Sadowski, H. W. Zandbergen, J.D. Thompson and R. J. Cava, Journal of Crystal Growth, in press (available online).
17. Quantum critical behavior in the heavy Fermion single crystal $Ce(Ni_{0.93}5Pd_{0.065})_2Ge_2$, C. H. Wang, J. M. Lawrence, A. D. Christianson, S. Chang, E. D. Bauer, K. Gofryk, F. Ronning, J. D. Thompson, K. J. McClellan, J. A. Rodriguez, J. W. Lynn, Journal of Physics: Conference Series, to be published.
18. Heavy Fermion Scaling: uranium versus cerium and ytterbium compounds, J M Lawrence, C H Wang, A D Christianson and E D Bauer, Journal of Physics: Condensed Matter **23** (2011), to be published. arXiv: 1101.3992.
19. Inelastic neutron scattering studies of the intermediate valence compound $CePd_3$, V.R. Fanelli, J.M. Lawrence, C.H. Wang, A.D. Christianson, E.D. Bauer, K.J. McClellan, E.A. Goremychkin, and R. Osborn, arXiv: 0908.4378.
20. Inelastic neutron scattering study of the intermediate valence compounds $CePd_3$ and $YbAl_3$, Victor Fanelli, Ph D thesis, University of California, Irvine, 2009.

Personnel and Collaborations for DOE Grant DE-FG02-03ER46036

An important aspect of this research grant has been training young scientists in the physics of correlated electron materials and in the techniques of neutron scattering. Andrew Christianson worked as a postdoc whose major contributions to the research were in the neutron scattering studies of the intermediate valence compound $YbAl_3$, the heavy Fermion compound $Ce_3Co_4Sn_{13}$, and the induced moment antiferromgnet Pr_3In. In addition, he made significant contributions to almost all of the other research performed under the grant. Christianson is now a scientific staff member in the neutron scattering group at Oak Ridge National Laboratory. Victor Fanelli carried out his Ph. D. research on neutron scattering studies of $CePd_3$ and on high magnetic field studies of Pr_3In. After serving as a postdoc at the National High Magnetic Field Laboratory's Pulsed Field Facility at Los Alamos, Fanelli has recently been hired as a scientific staff member at the Lujan Center at Los Alamos. Cui-Huan Wang worked as a postdoc on this research; her major contributions were in neutron scattering studies of the heavy Fermion compounds Ce_3In and Ce_3Sn and of the actinide heavy Fermion compounds UCo_2Zn_{20}, URu_2Zn_{20} and UMn_2Al_{20}. She is currently a postdoc in the neutron scattering group at Oak Ridge National Laboratory.

Our primary collaboration has been with Eric Bauer and Joe Thompson in the condensed matter physics group MPA-CMMS at Los Alamos. Bauer guided Christianson, Fanelli, and Wang in crystal growth and Thompson guided them in the study of basic properties such as specific heat and susceptibility of the relevant compounds.

Key collaborators for the neutron experiments have been Ray Osborn and Eugene Goremychkin at Argonne National Laboratory, Jerel Zaretsky at Oak Ridge, Chris Frost at ISIS, Jason Gardner at NIST, and Frans Trouw at Los Alamos.